JBIC Journal of Biological Inorganic Chemistry (2018) 23:725–738
https://doi.org/10.1007/s00775-018-1562-8

ORIGINAL PAPER

Characterization of the complex between native and reduced bovine serum albumin with aquacobalamin and evidence of dual tetrapyrrole binding

Ilia A. Dereven'kov[1] · Luciana Hannibal[2] · Sergei V. Makarov[1] · Anna S. Makarova[3] · Pavel A. Molodtsov[1] · Oskar I. Koifman[1,3]

Received: 26 November 2017 / Accepted: 25 April 2018 / Published online: 2 May 2018

Abstract

Serum albumin binds to a variety of endogenous ligands and drugs. Human serum albumin (HSA) binds to heme via hydrophobic interactions and axial coordination of the iron center by protein residue Tyr161. Human serum albumin binds to another tetrapyrrole, cobalamin (Cbl), but the structural and functional properties of this complex are poorly understood. Herein, we investigate the reaction between aquacobalamin (H_2OCbl) and bovine serum albumin (BSA, the bovine counterpart of HSA) using Ultraviolet–Visible and fluorescent spectroscopy, and electron paramagnetic resonance. The reaction between H_2OCbl and BSA led to the formation of a BSA-Cbl(III) complex consistent with N-axial ligation (amino). Prior to the formation of this complex, the reactants participate in an additional binding event that has been examined by fluorescence spectroscopy. Binding of BSA to Cbl(III) reduced complex formation between the bound cobalamin and free cyanide to form cyanocobalamin (CNCbl), suggesting that the β-axial position of the cobalamin may be occupied by an amino acid residue from the protein. Reaction of BSA containing reduced disulfide bonds with H_2OCbl produces cob(II)alamin and disulfide with intermediate formation of thiolate Cbl(III)-BSA complex and its decomposition. Finally, in vitro studies showed that cobalamin binds to BSA only in the presence of an excess of protein, which is in contrast to heme binding to BSA that involves a 1:1 stoichiometry. In vitro formation of BSA-Cbl(III) complex does not preclude subsequent heme binding, which occurs without displacement of H_2OCbl bound to BSA. These data suggest that the two tetrapyrroles interact with BSA in different binding pockets.

Keywords Cobalamin · Serum albumin · Cyanide · Thiols · Reaction mechanisms

Abbreviations

BSA	Bovine serum albumin
Cbl	Cobalamin
CNCbl	Cyanocobalamin
DEPC	Diethyl pyrocarbonate
DMBI	5,6-dimethylbenzimidazole
H_2OCbl	Aquacobalamin
HSA	Human serum albumin

Electronic supplementary material The online version of this article (https://doi.org/10.1007/s00775-018-1562-8) contains supplementary material, which is available to authorized users.

✉ Ilia A. Dereven'kov
derevenkov@gmail.com

[1] Institute of Macroheterocyclic Compounds, Ivanovo State University of Chemistry and Technology, Sheremetevskiy Str. 7, Ivanovo 153000, Russian Federation

[2] Laboratory of Clinical Biochemistry and Metabolism, Department for Pediatrics, Medical Center, University of Freiburg, Mathildenstr. 1, 79106 Freiburg, Germany

[3] G. A. Krestov Institute of Solution Chemistry of the Russian Academy of Sciences, Academicheskaya Str 1, Ivanovo 153045, Russian Federation

Introduction

Cobalamins (Cbls, vitamin B_{12}), the vitamins with the most complex structure, are widespread in the Nature's group of metal-containing cofactors. Their key structural feature is the presence of cobalt ion (viz., Co(III), Co(II) and Co(I)) surrounded by corrin macrocycle (Fig. 1). In aquacobalamin (H_2OCbl), axial positions are occupied by 5,6-dimethylbenzimidazole nucleotide (a lower (α) axial ligand) and a water molecule (an upper (β) axial ligand) [1]. The bound water molecule in the complex is relatively labile and can be

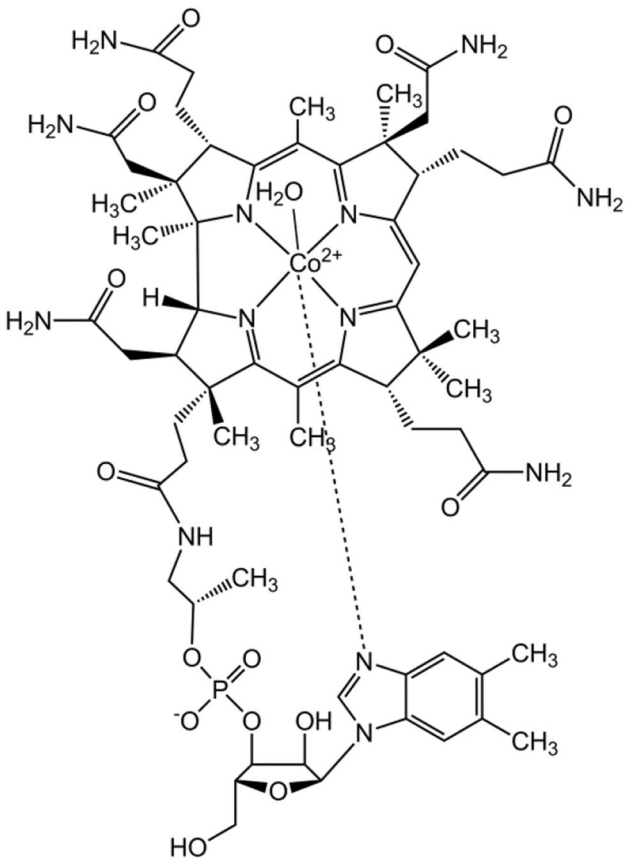

Fig. 1 Structure of aquacobalamin

substituted by various endo- and exogenous ligands [2, 3]. An interaction of non-toxic H_2OCbl with cyanide leading to the formation of cyanocobalamin (CNCbl) underlies its use as an antidote to this toxin [4, 5].

The interaction of Cbls with proteins represents an important part of their biological functions [6, 7]. Cbls are common cofactors of various enzyme systems. In mammals, Cbl-dependent proteins methionine synthase and methylmalonyl-CoA mutase catalyze the synthesis of methionine from homocysteine and the isomerization of methylmalonyl-CoA to succinyl-CoA, respectively [8]. The transport of Cbls and their intracellular processing involves a sequence of specific proteins: the transport of Cbls from the oral cavity to the duodenum is carried out by haptocorrin [6, 9], after that intrinsic factor transfers Cbls to enterocytes [6, 9] and then transcobalamin escorts them to the cells [6, 9–11]. Inside the cells, Cbls can be subjected to β-axial deligation by the CblC-protein [12–15].

Serum albumins are the most abundant proteins in the circulatory system [16]. Human serum albumin in circulation is found in concentrations between 527 and 783 micromolar [17]. They act as transporters of numerous endo- and exogenous compounds. Serum albumins are capable of binding and transferring fatty acids [18, 19], bilirubin [20, 21], porphyrins [22–24], steroids [25, 26] and other compounds. They are also capable of binding metal ions and drugs at specific sites [27, 28]. Binding of drugs with plasma proteins is an important pharmacological characteristic: the tight binding reduces the active concentration of the drug in the blood plasma and leads to its slow release.

Due to its readily commercial availability and high structure conservation with serum albumins from other species, bovine serum albumin (BSA) is frequently used as a general model of serum albumins in various in vitro studies. Bovine serum albumin presents 75% amino acid residue identity compared to human serum albumin. The structure of BSA contains 583 amino acid residues, in particular, it includes 35 cysteines (i.e., 34 cysteines are oxidized and form intramolecular disulfide bridges and one cysteine is in thiol form), 4 methionines, 2 tryptophans, 17 histidines, 58 lysines, 23 arginines, 20 tyrosines and others [29].

The interaction of CNCbl with serum albumins has been studied in several works [30–32]. It was shown that CNCbl is capable of quenching fluorescence of human (HSA) and bovine serum albumins. In the case of HSA, the quenching occurs via the dynamic mechanism [30], whereas CNCbl quenches BSA fluorescence via the static or combined mechanism [31]. It is noted that BSA structure is significantly altered during the formation of complex with CNCbl [32]. H_2OCbl is also capable of interacting with serum albumin, i.e., to form a nitrogenous complex [33–36]. The Co(III)-BSA coordination was reported to be tight and proposed to occur via histidine residues [34, 35]. These studies provided information on the interaction of BSA with H_2OCbl under equilibrium conditions [34, 35], and one of them [34] utilized concentrations of H_2OCbl exceeding those of BSA, which lacks biological relevance. Under such conditions, one study identified a binding stoichiometry of 1.4 mol of H_2OCbl per mole of BSA, and this ratio was shown to increase up to 5–16 mol of H_2OCbl per mole of BSA with temperature, time and the addition of urea [34]. The other investigation determined this stoichiometry to be 0.5 mol H_2OCbl per mol of BSA [35]. The complexation of H_2OCbl with BSA was also shown using ^{31}P NMR spectroscopy [36] (binding ligands on Co(III) affects chemical shifts of ^{31}P). While advances have been made, our knowledge of the kinetic and structural features involved in the binding of albumin to vitamin B_{12} is very limited, which hampers our understanding of the potential biological relevance of this interaction. For example, binding of H_2OCbl to BSA via other nitrogenous groups (e.g., of amino groups), the kinetics of BSA-Cbl(III) complex formation, and whether H_2OCbl binding disrupts the known association of the tetrapyrrole heme with BSA have not been examined. Herein, we demonstrate that: (i) bovine serum albumin binds to H_2OCbl to form a stable complex that features N-coordination with

contribution of a lysine amino group, (ii) binding of BSA to H_2OCbl occurs with forward and reverse reaction rates of (128 ± 4) M^{-1} min^{-1} and (0.015 ± 0.002) min^{-1}, respectively, which yield a binding constant of 8500 M^{-1}, (iii) binding of BSA to H_2OCbl limits the ability of the cobalamin to coordinate cyanide to form cyanocobalamin, suggesting that the β-axial position of cobalamin is occupied by an amino acid residue from the protein, (iv) pre-reduction of disulfide bonds in BSA and subsequent reaction with aquacobalamin leads to reduction of the micronutrient to cob(II)alamin, and (v) binding of aquacobalamin to BSA requires a molar excess of protein and does not impair the protein's ability to bind heme, suggesting the existence of distinct binding modes for each tetrapyrrole.

Experimental section

Reagents

Hydroxocobalamin hydrochloride (Sigma; HOCbl; ≥ 96%), bovine serum albumin (Sigma or Acros Organics; heat shock fraction, pH 5.2; ≥ 96%) and glutathione (Sigma; GSH; ≥ 98%) were used without additional purification. Oxygen-free argon was used to deoxygenate reagent solutions.

Buffer solutions (acetate, phosphate and borate) were used to maintain pH during the measurements. Ionic strength was adjusted to 0.2 M using $NaNO_3$ in all measurements.

The pH values of solutions were determined using Multitest IPL-103 pH-meter (SEMICO) equipped with ESK-10601/7 electrode (Izmeritelnaya tekhnika) filled by 3.0 M KCl solution. The electrode was preliminarily calibrated using standard buffer solutions (pH 1.65–12.45).

Concentrations of Cbl stock solutions were determined using UV–Vis spectroscopy via a conversion of Cbl to its dicyano-form (extinction coefficient is 30400 M^{-1} cm^{-1} at 368 nm [37]).

Reduction of disulfide bonds in BSA

Reduction of disulfide bonds in BSA was performed using 0.2 M sodium borohydride added to a 0.002 M BSA solution, for 12 h. This method is advantageous for this study over other ways of disulfide bond reduction in BSA (e.g., using dithiothreitol or tris(2-carboxyethyl)phosphine), since there is no borohydride or other redox active products of its decomposition in the system by the end of the reduction. The content of thiol groups in BSA was determined using Ellman's reagent at pH 8, 25 °C [38]. Under our experimental conditions, this reduction protocol leads to the formation of 6 thiol groups per molecule of albumin (three disulfide bonds were reduced).

Preparation of BSA, heme and cobalamin stock solutions for end-point binding experiments

A stock solution of 1 mM BSA (Sigma, product Nr. 7906) was prepared by dissolving lyophilized BSA in buffer EPPS (40 mM, pH 7.4) supplemented with 150 mM NaCl and 10% glycerol. Solutions of BSA were prepared freshly and kept on ice during the course of the experiments. Aquacobalamin stock solutions were prepared and the concentration was measured as described above. Hemin solutions were prepared by dissolving solid hemin in 0.1 N NaOH and 5% DMSO. Addition of DMSO prevents the formation of porphyrin dimers [39]. The concentration of heme was determined spectrophotometrically using an absorption extinction coefficient of 58.4 mM^{-1} cm^{-1} at 385 nm [40].

Buffer exchange of BSA solutions

For buffer-exchange reactions, spin-filters with a molecular weight cut-off of 30 kDa were handled as suggested by the manufacturer (Amicon). Briefly, spin-filters were first hydrated with 0.5 mL mQ H_2O by one cycle of centrifugation at 13,000 rpm, 10 min, at 4 °C. The spin-filters were then equilibrated with 0.5 mL buffer (EPPS (40 mM, pH 7.4) supplemented with 150 mM NaCl and 10% glycerol), by performing one more cycle of centrifugation at 13,000 rpm, 10 min, at 4 °C. The filtrates were discarded, and the appropriate protein solution (BSA, BSA-Cbl(III), BSA-heme, BSA-heme +Cbl, as needed) were loaded onto the spin-filters. Buffer-exchange was performed by successive centrifugation cycles, disposal of the filtrate, and addition of buffer to wash-off unwanted, unreacted diethylpyrocarbonate (DEPC), Cbl or heme (see experiments outlined below). Free Cbl and free heme eluted in the filtrate, whereas BSA, BSA-heme and BSA-Cbl(III) complexes were retained in the filter and utilized for further analysis.

Ethoxylation of BSA with DEPC

The modification of His residues and to a much lesser extent of Lys and Tyr residues in proteins has been investigated extensively using DEPC [41]. An aliquot of 1 mM BSA prepared as described above was incubated with 150 mM DEPC, for 2 h on ice. Removal of unreacted DEPC was performed by applying 5 cycles of buffer exchange using spin filters with a molecular weight cut-off of 30 kDa (Amicon).

End-point binding analysis of the interactions of BSA with the tetrapyrroles heme and aquacobalamin

Formation of complexes between BSA and the respective tetrapyrroles was monitored by direct mixing of protein to tetrapyrrole in a 1.1–1 molar ratio, with subsequent recording of the UV–Visible spectrum between 250 and 700 nm after 10 min. Complexes of BSA with each tetrapyrrole were also formed by incubating the reactants (1 mM BSA with 1 mM heme or 1 mM aquacobalamin) for 1 h, at room temperature (20 ± 1 °C), followed by 5 cycles of buffer-exchange to eliminate unbound tetrapyrrole. UV–Visible spectra of the buffer-cleared complexes were recorded to examine maximum tetrapyrrole loading in each case.

UV–Visible spectroscopy

Ultraviolet–Visible (UV–Vis) spectra were recorded on a cryothermostated (± 0.1 °C) Cary 50 UV–Vis spectrophotometer in quartz cells.

Fluorescence spectroscopy

Fluorescence emission spectra were recorded on a Shimadzu RF-6000 spectrofluorophotometer in non-fluorescent cells under aerobic conditions at room temperature (19 ± 1 °C). The excitation wavelength was 280 nm, the excitation and emission bandwidths were 1.5 and 20.0 nm, respectively. The fluorescence intensities were corrected with respect to the inner filter effect. Dynamic quenching was examined as described by Stern–Volmer Eq. (1) [32].

$$\frac{F_0}{F} = 1 + K_Q \tau_0 [Q] = 1 + K_{SV}[Q] \quad (1)$$

where F_0 and F are fluorescence intensities in the absence and in the presence of a quencher. K_Q is quenching rate constant, $M^{-1}\ s^{-1}$. K_{SV} is the Stern–Volmer fluorescence quenching constant, M^{-1}. τ_0 is the average fluorescence lifetime of the BSA molecule without quencher, s; [Q] is the quencher concentration, M. Considering formation of a stable complex between BSA and H_2OCbl, we determined equilibrium constants for this interaction using Eq. (2) [32].

$$\log\left(\frac{F_0 - F}{F}\right) = \log K + n \cdot \log [Q] \quad (2)$$

where F_0 and F are fluorescence intensities in the absence and in the presence of a quencher. K is the equilibrium constant for the binding quencher by BSA, M^{-n}. n is the number of binding sites. [Q] is the quencher concentration, M.

EPR spectrometry

EPR spectra were measured at liquid nitrogen temperature at 96.5 K, with a BRUKER-BIOSPIN EMX spectrometer operating in the X-band (9.5 GHz). The EPR parameters were: modulation frequency of 100 kHz, microwave power of 1 mW, modulation amplitude of 3 G, time constant of 40.96 ms, sweep time of 180.22 s, sweep width of 4000G with a central field of 2500 G, resolution of 4096 points and one scan.

Experimental data were analyzed using Origin 7.5 software.

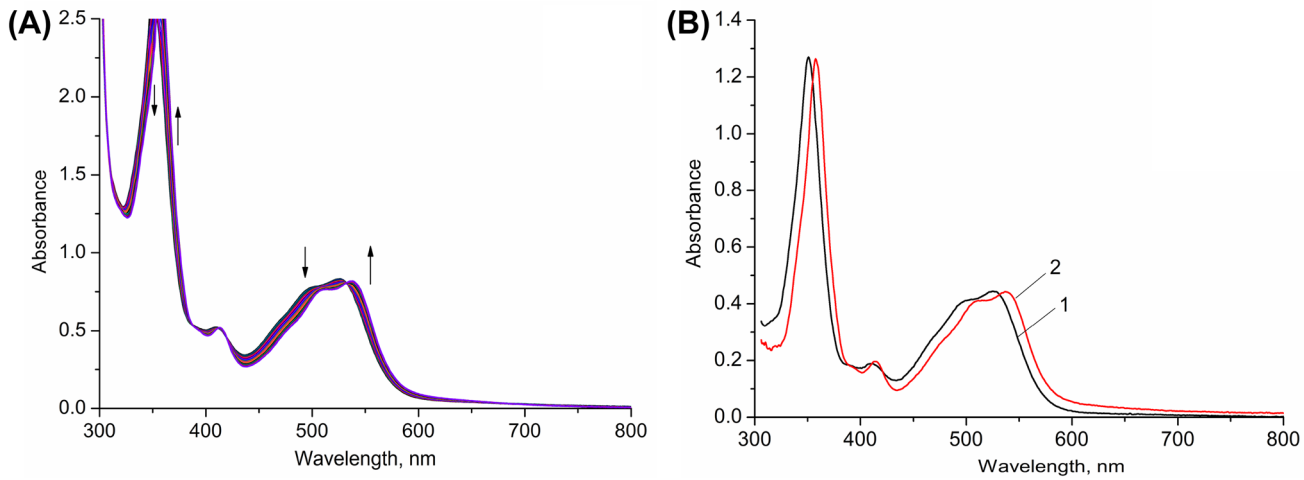

Fig. 2 UV–Vis spectra of the reaction between H_2OCbl (8×10^{-5} M) and BSA (9×10^{-4} M) at pH 7.2, 37 °C (**a**). UV–Vis spectra of H_2OCbl (1; 5×10^{-5} M) and BSA-Cbl(III) complex (2; 5×10^{-5} M) at pH 7.2, 37 °C (**b**)

Results and discussion

Aquacobalamin binds to BSA with distinct spectral features, stoichiometry and pH dependence

The reaction between H_2OCbl and BSA was accompanied by a slight red-shift in the UV–Vis spectrum compared to free H_2OCbl, as shown in Fig. 2. Increases in absorbance intensity are observed at 370 and 550 nm, with isosbestic points appearing at 353, 389, 411 and 532 nm.

It should be noted that these UV–Vis spectral changes are not characteristic for binding thiols by Cbl(III) [42] (i.e., UV–Vis spectrum of thiolato-Cbl(III) exhibits maxima at 373, 535 and 560 nm) and likely correspond to binding of a weaker axial ligand such as nitrogen (amino) group. Similar changes were observed during the complexation of amino acids on Cbl(III) via amino group [43]. We found that Cbl(III) does not form complexes with amide groups of asparagine and glutamine (Cbl(III) binds asparagine and glutamine via amino groups [43]) and with guanidine that mimics a side chain of arginine. To determine the type of group taking part in the binding, we recorded UV–Vis spectra of the reactions of H_2OCbl with ethylenediamine and imidazole. The reaction with amino group in ethylenediamine mimics BSA binding via terminal amino group or amino group of lysine side chain and the interaction with imidazole – binding via histidine side chain. We found that reactions of Cbl(III) with ethylenediamine and imidazole (Fig. 3) at pH 7.2 are accompanied by UV–Vis spectral changes similar to those collected in the course of reaction with BSA (Fig. 2). The interaction with imidazole proceeds within several seconds, but the reaction with ethylenediamine—within several tens of minutes as the reaction with BSA. Therefore, these results suggest that binding of BSA with Cbl(III) occurs via an amino group.

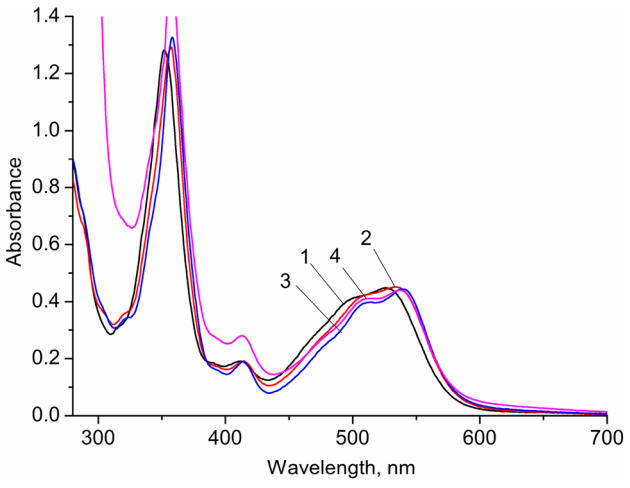

Fig. 3 UV–Vis spectra of H_2OCbl (5×10^{-5} M; 1) and complexes of Cbl(III) (5×10^{-5} M) with ethylenediamine (3×10^{-2} M; 2), imidazole (3×10^{-2} M; 3) and BSA (9×10^{-4} M; 4) incubated at pH 7.2, 37 °C for 1 h

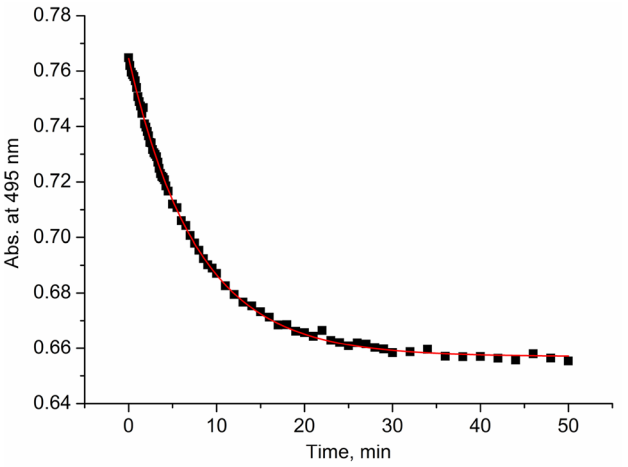

Fig. 4 Typical kinetic curve of the reaction between H_2OCbl (8×10^{-5} M) and BSA (9×10^{-4} M) at pH 7.2, 37 °C

Next, we studied the kinetics of the reaction between H_2OCbl and an excess of BSA. A typical time-course curve is provided in Fig. 4. The binding event can be best described by an exponential equation that is first order with respect to the concentration of H_2OCbl.

Observed rate constants of the reaction ($k_{obs.1}$) with varying concentrations of BSA were also determined. The $k_{obs.1}$ exhibited a linear dependence with BSA concentration, which indicates first order with respect to BSA and has a positive *Y*-intercept. For the ligand exchange reactions with

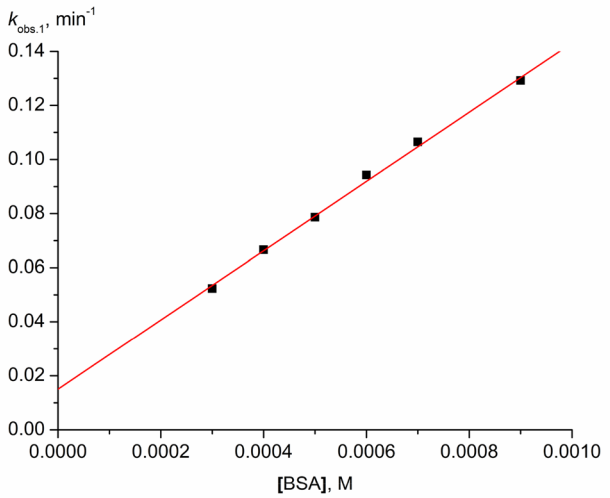

Fig. 5 Plot of observed rate constants ($k_{obs.1}$) of the reaction between H_2OCbl and BSA versus BSA concentration at pH 7.2, 37 °C

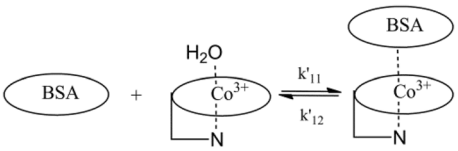

Scheme 1 Complex formation between BSA and H_2OCbl

H_2OCbl, the intercept can be explained by a reverse reaction (i.e., a dissociation of formed complex). At pH 7.2, 37 °C values of rate constants of forward (k'_{11}) and reverse (k'_{12}, *Y*-intercept in Fig. 5) reactions (Scheme 1) are (128 ± 4) M^{-1} min^{-1} and (0.015 ± 0.002) min^{-1}, and value of equilibrium constant determined as k'_{11}/k'_{12} ratio is 8500 M^{-1} (Fig. 5). This value differs from a previously reported value of 1.8×10^4 M^{-1} at pH 7.4, 37 °C using equilibrium dialysis [34]. A major difference concerns the experimental conditions. Our study was performed utilizing varying concentrations of BSA, with [BSA] > [H_2OCbl], and this condition was selected for two reasons: (a) BSA is the ligand in our reaction, providing a nitrogen atom for the axial coordination to H_2OCbl, so we thought it reasonable to vary the concentration of ligand, BSA, while keeping H_2OCbl constant; and (b) [BSA] > [H_2OCbl] are conditions that more closely resemble the biological context in which this binding event could occur. In blood, the concentration of BSA is 0.5–0.8 mM [17], whereas the concentration of cobalamin ranges from 200 to 800 pM, with maximum levels of c.a. 2500 pM reached only under treatment for severe vitamin B_{12} deficiency [44]. The study of Taylor and Hanna [34] consisted of equilibrium dialysis where [BSA] ≪ [H_2OCbl]. These experimental conditions facilitate the occurrence of non-specific binding of H_2OCbl to BSA, which the authors themselves acknowledged in their publication [34]. Thus, the previously published binding constant of 1.8×10^4 M^{-1} likely represents a blend of specific and non-specific associations of H_2OCbl to BSA.

Examination of the dependence of the direct reaction, k'_{11}, on pH is shown in Fig. 6. Binding of BSA to H_2OCbl exhibits a bell-shaped profile that can be explained by the influence of acid–base properties of both reactants on the kinetics.

One of the pK_a values determining the profile of pH-dependence is pK_a of H_2OCbl (7.8 at 25 °C [42]). Figure 6. indicates that the second pK_a related to BSA is expected to be more than 7.8. Since mean pK_a value of histidine moieties for various proteins is 6.6 at 25 °C [45], it can be assumed that this equilibrium involves lysine, a more basic acid, and corresponds to deprotonation of its side chain amino group (mean pK_a value of side chain amino group of lysine is 10.5 whereas the value for terminal amino group is 8.0 at 25 °C [45]).

Dependence of rate constants of reverse reaction (k'_{12}) on pH is shown in Fig. 7. The dependence has profile of S-shaped curve. Fitting this plot with use of a sigmoid curve equation produces pK_a = 8.8 ± 0.1 that is close to pK_a of a lysine amino group.

The UV–Visible spectral and kinetic analysis of the binding of BSA with H_2OCbl suggests the mechanisms shown in Scheme 2. Two acid–base equilibria are characteristic for initial reactants: protonation of hydroxocobalamin and protonation of a NH_2–group of protein. Hydroxocobalamin is inactive in ligand exchange reactions and only H_2OCbl is capable of participating in these reactions. Probably, both forms of amino group interact with H_2OCbl, however, –NH_2 form is a stronger nucleophile and reacts with H_2OCbl at a

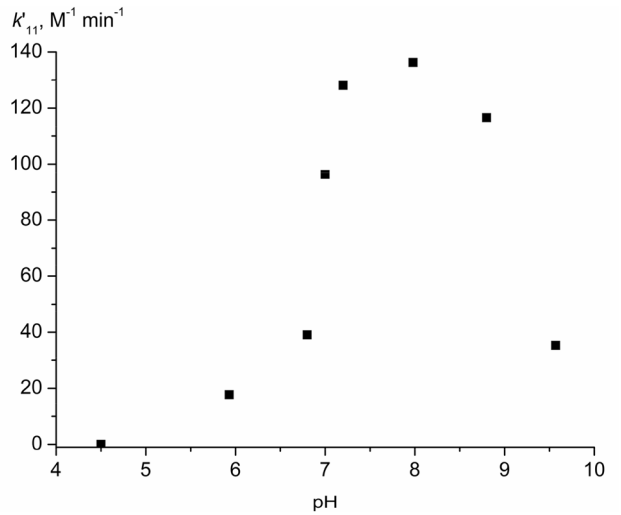

Fig. 6 Plot of rate constant of forward reaction (k'_{11}) between H_2OCbl and BSA versus pH at 37 °C

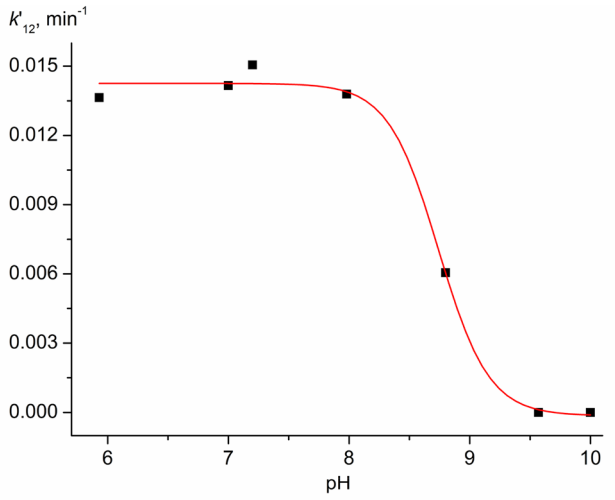

Fig. 7 Plot of rate constant of reverse reaction (k'_{12}) between H_2OCbl and BSA versus pH at 37 °C

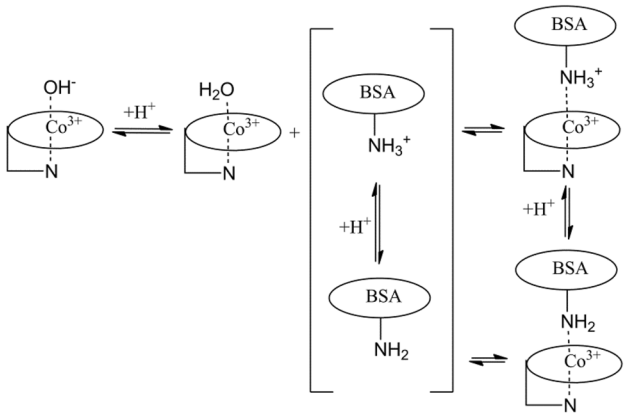

Scheme 2 Mechanism of reaction between H_2OCbl and bovine serum albumin

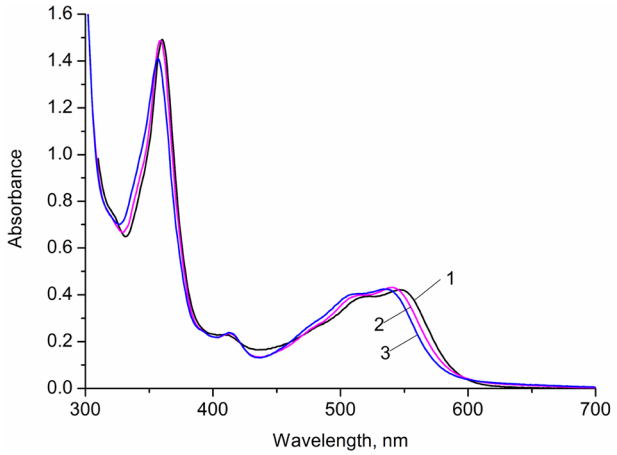

Fig. 8 UV–Vis spectra of CNCbl (5×10^{-5} M) (1), product of the reaction between CN^- (5×10^{-5} M) and H_2OCbl (5×10^{-5} M) incubated in the presence of BSA (4×10^{-4} M) for 1 h (2; time after addition of cyanide – 10 min), and the BSA/H_2OCbl mixture incubated for 1 h (3). pH 7.2, 37 °C

higher rate. A protonated amino group is weakly bound to Co(III) and it dissociates more rapidly than $–NH_2$ form. It should be noted that this binding mode differs from suggested earlier one involving histidine [34, 35]. Proof of His involvement was provided by competition studies using Cd^{2+}, which bind to His residues of BSA [35]. Cd^{2+} has a binding affinity for His residues of BSA of 6.3×10^2 M^{-1} [46]. Interestingly, the authors noted that Cd^{2+} was effective in preventing formation of a 1:1 BSA-Cbl(III) complex, but ineffective at displacing 0.4 equivalents of H_2OCbl bound to BSA from the initial 1:1 molar mixture of H_2OCbl and BSA [35]. This suggests that there are at least two distinct binding modes in the association of H_2OCbl to BSA, only one of which is disrupted by Cd^{2+}. Another possibility is the occurrence of intramolecular ligand exchange reactions, where neighbor Lys and His residues in the protein could compete and alternate for the coordination of the Co center, depending on the microenvironment and conformational arrangement of the protein. Unequivocal resolution of this conundrum requires structural elucidation of the BSA-Cbl(III) complex. Unfortunately, our attempts to obtain crystals of BSA-Cbl(III) complex have been unsuccessful. While our studies do not exclude the participation of His residues in the associations of H_2OCbl with BSA, our results along with previous literature suggest that such binding events predominantly occur at $H_2OCbl \gg$ BSA, are non-specific, and occur under conditions not relevant in biology.

Pre-formation of a BSA-Cbl(III) complex reduces the reactivity of the bound cobalamin with cyanide

To further characterize the properties of the BSA-Cbl(III) complex, we examined whether pre-formation of a complex between H_2OCbl and BSA has an impact in subsequent binding of the cobalamin molecule to free cyanide. Reaction of an alkaline solution of cyanide with BSA-H_2OCbl complex has been investigated earlier [34]. Addition of cyanide was shown to result in dissociation of cobalamin from the complex [34]. However, data on the interaction at physiological pH, where cyanide exists mostly in the protonated, less nucleophilic HCN-form, are lacking.

Figure 8 shows that cyanide influences the spectra of an aquacobalamin—BSA mixture. Simultaneous mixing of H_2OCbl with BSA and cyanide did not affect the conversion of Cbl(III) to CNCbl. In contrast, prolonged pre-incubation of H_2OCbl in the presence of BSA decreased the yield of conversion of Cbl(III) to CNCbl upon addition of free cyanide (Fig. S1). Decrease in the conversion degree of Cbl(III) to CNCbl is pronounced only after several minutes of incubation of H_2OCbl with BSA and the lowest yield of CNCbl is observed after the incubation for 30 min and more at 37 °C. The prolonged pre-incubation of BSA with H_2OCbl also slightly reduced the observed rate constant at which cyanide binds to Cbl(III) to form CNCbl. Thus, the observed rate constants for cyanide (0.5 mM) binding to free H_2OCbl and H_2OCbl incubated with BSA (0.9 mM) for 30 min are 0.09 and 0.07 s^{-1} (pH 7.2, 37 °C), respectively (Fig. S1).

The weak influence of BSA on the rate of reaction of aquacobalamin with cyanide can be explained by the involvement in the reaction of only H_2OCbl that is present in solution in the equilibrium with amino complex which reacts with cyanide much slower. This equilibrium is establishing relatively slow. Reaction of H_2OCbl with cyanide is characterized by high equilibrium constant [47] that finally will shift Cbl(III) in the presence of BSA to CNCbl. It is also possible that binding of Cbl leads to heterogeneous BSA-Cbl complex pools. For example, a fraction of the bound Cbl may exist as H_2OCbl, without any axial ligands from the

protein displacing the water group, whereas another fraction may involve direct coordination of a N-containing ligand, such as Lys, making the reaction of the cobalt center with cyanide less favorable.

Therefore, the formation of complex between Cbl(III) and BSA can decrease the number of coordination centers available for ligand exchange. The effect of BSA on cyanide binding by Cbl(III) differs from that of thiocyanate binding to Cbl(III) [48]: thiocyanate retards the reaction, but it does not influence the yield of CNCbl formation. This can be explained by lower lability of bulk of the BSA-Cbl(III) complex in which the upper axial ligand of the Cbl molecule cannot be directly substituted by CN^- in contrast to the more labile thiocyanate ligand.

Studies on the reaction between aquacobalamin and bovine serum albumin using fluorescent spectroscopy

UV–Visible spectroscopy showed that addition of an excess of H_2OCbl to BSA does not induce any changes in the spectrum within the first minutes after mixing (Fig. S2). The same results were obtained when an excess of BSA was added to an H_2OCbl solution. Nevertheless, several interactions (electrostatic, hydrophobic, hydrogen bonds formation and others) that do not affect chromophores of reactants likely proceed within this time. These interactions can be studied using fluorescent spectroscopy by monitoring Trp fluorescence quenching in the protein (335 nm) upon binding to its ligand.

We established that addition of H_2OCbl results in quenching fluorescence of BSA at 335 nm (Fig. 9). It should be noted that not only decrease in intensity of fluorescence emission peak occurs, but the peak is distinctly split, as was observed for the interaction between CNCbl and BSA [32] (Fig. S3). This can occur upon changes in the environment surrounding tryptophan units in the protein: reaction between CNCbl and BSA leads to folding polypeptide chains in close proximity of one of tryptophan units that decreases polarity of surrounding environment [32].

Fluorescence quenching of Trp induced by cobalamin binding has been proposed to occur via two possible mechanisms: static and dynamic. The static mechanism proceeds via the formation of a stable complex between BSA and cobalamin, whereas the dynamic binding route involves rapid contact between reactants within the lifetime of the excited state.

Our experimental results in the form of a Stern–Volmer plot are shown in Fig. 10. A linear dependence was documented, suggestive of a single type of quenching mechanism. The value of the dynamic fluorescence quenching constant is $K_{SV} = (6.5 \pm 0.4) \cdot 10^4\ M^{-1}$ at (19 ± 1) °C, pH 7.0. Since the value of τ_0 is ca. 10^{-8} s [49], K_Q is $6.5 \cdot 10^{12}\ M^{-1}\ s^{-1}$. This value substantially exceeds the maximum value of the dynamic quenching rate constant for proteins ($2 \cdot 10^{10}\ M^{-1}\ s^{-1}$ [50]) that can result from complex formation between BSA and H_2OCbl. Thus, our experimental results are in line with the proposal that BSA fluorescence quenching by H_2OCbl proceeds via a static mechanism, as it has been described for CNCbl in this concentration range [31, 32].

Fitting the plot of $\log((F_0 - F)/F)$ versus $\log[H_2OCbl]$ (Fig. 11) gives values $n = (1.23 \pm 0.01)$, $\log K = (5.9 \pm 0.1)$. For the reaction between CNCbl and BSA performed under the same conditions, these values are $n = (1.01 \pm 0.03)$, $\log K = (4.7 \pm 0.2)$ (Figs. S4,S5). Thus, regardless of the chemical nature of the β-axial ligand of the cobalamin

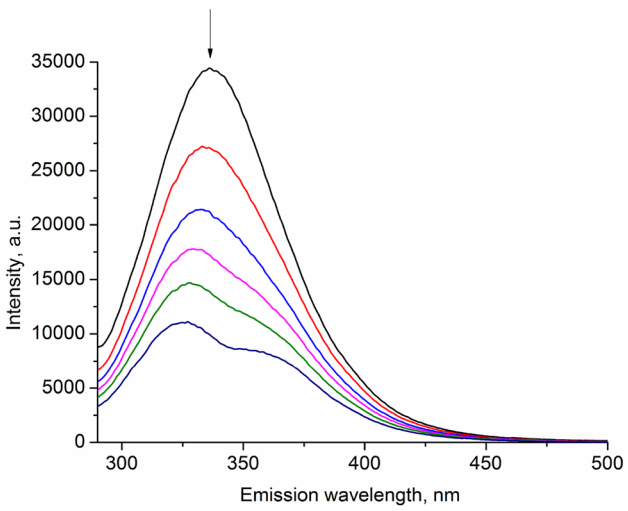

Fig. 9 Fluorescence emission spectra of BSA (1×10^{-6} M) in the presence of H_2OCbl at pH 7.0, room temperature (19 ± 1 °C)

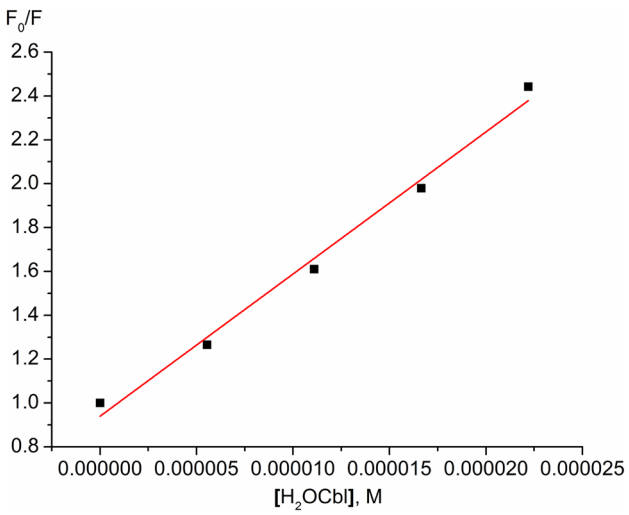

Fig. 10 Stern–Volmer plot for the interaction between BSA (1×10^{-6} M) and H_2OCbl at pH 7.0, (19 ± 1) °C

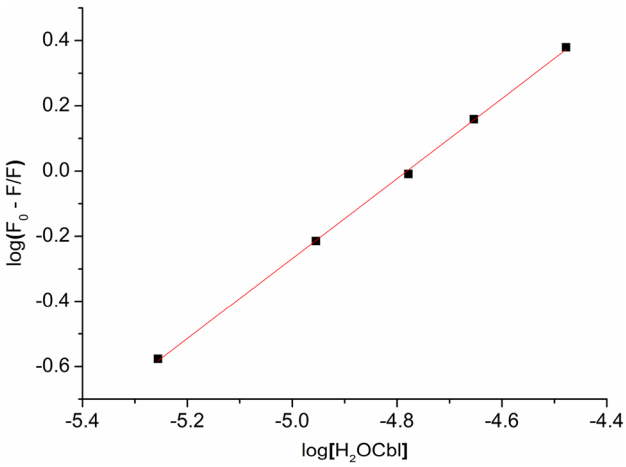

Fig. 11 Plot of $\log((F_0 - F)/F)$ versus $\log[H_2OCbl]$ for the reaction between BSA (1×10^{-6} M) and H_2OCbl at pH 7.0, (19 ± 1) °C

moiety, fluorescence studies indicate a stoichiometry of association of 1:1 for BSA:Cbl.

These results indicate that an additional equilibrium precedes the amino complex formation between Cbl(III) and BSA, and this could also mean mixed binding states, that include pools with and without axial ligation. Results from a study with CNCbl showed that complex formation with BSA likely involves via $\pi - \pi$-stacking [32]. The bulk and spatial arrangement of the cobalamin molecule make it at a first glance counter-intuitive that $\pi - \pi$-stacking interactions may assist in its binding to proteins that lack a canonical cobalamin binding site. As discussed above from literature and our experiments using UV–Visible spectrophotometry, distinct binding association modes occur for BSA-Cbl(III) depending on the relative concentration of reactants. It is plausible that prior to changes in the axial coordination environment of the cobalamin molecule, conformational rearrangement occurs within the protein to stabilize the bound tetrapyrrole via hydrophobic interactions and hydrogen bond formation. Additionally, comparison of equilibrium constants of BSA binding by CNCbl and H_2OCbl shows that H_2OCbl is more tightly bound. This can be explained by the difference in charge of the complexes: H_2OCbl is positively charged (+ 1) whereas CNCbl is neutral.

Pre-reduced bovine serum albumin exhibits cobalamin reductase activity

The commercial BSA sample contains 0.5 thiol groups per protein molecule as was determined by the Ellman's assay (there is only one free thiol group in native BSA molecule [17, 51]). The thiol groups of commercial, untreated BSA did not react with H_2OCbl, probably, due to sterical hindrances. To gain further insight into the molecular proximity of the albumin and the cobalamin moiety, we investigated the interaction of H_2OCbl with pre-reduced BSA.

As seen in Fig. 12, the interaction of H_2OCbl with reduced BSA includes several consecutive stages. The first phase of the reaction led to a reduction in peak intensity at 350 and 525 nm and an increase in absorbance at 366–464 and at 545–625 nm (Fig. 12a). A second phase is characterized by a decrease in absorbance at 355 and 530 nm and appearance of a new wavelength maximum at 475 nm (Fig. 12b). UV–Vis spectra collected during the first step are similar to those observed during the formation of

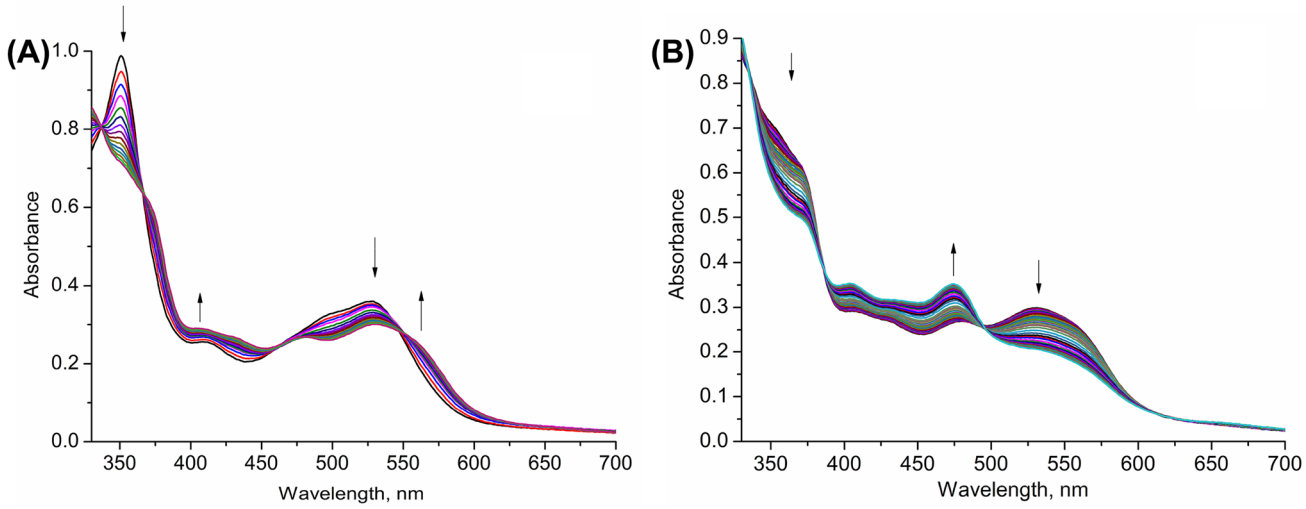

Fig. 12 UV–Vis spectra of the first (**a**) and following (**b**) stages of the reaction between H_2OCbl (4×10^{-5} M) and BSA (4×10^{-4} M) containing reduced disulfide bonds (6 thiol groups per BSA molecule) at pH 7.1, 25 °C

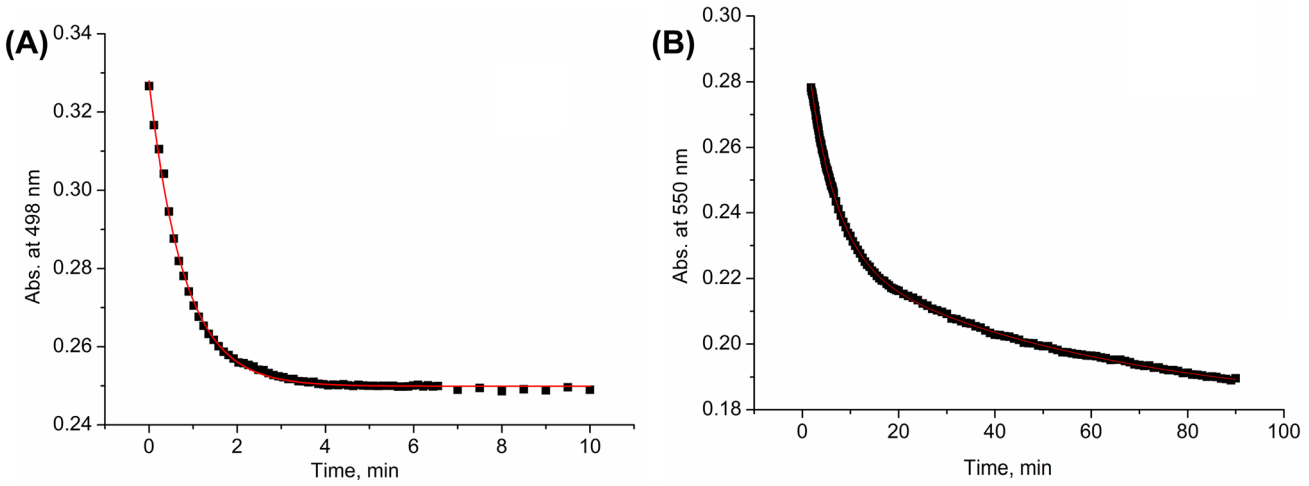

Fig. 13 Typical kinetic curves of the first (**a**) and following (**b**) steps of the reaction between H_2OCbl (4×10^{-5} M) and BSA (4×10^{-4} M) containing reduced disulfide bonds (6 thiol groups per BSA molecule) at pH 7.1, 25 °C

thiolato-Cbl(III) [42], and the spectrum of the final product after the second step coincides with that of Cbl(II) [48].

To confirm these results, we monitored formation of Cbl(II) by EPR spectrometry. EPR spectra of a mixture of H_2OCbl with reduced BSA recorded after incubation for 30 min and 4 h coincides with that of authentic Cbl(II) (Fig. S6).

We next examined the kinetics of reaction between H_2OCbl and an excess of reduced BSA. Typical kinetic curves are shown in Fig. 13. Kinetic curves of the first step (formation of thiolatocobalamin intermediate) are described by an exponential equation (Fig. 13a) that indicates the first order with respect to cobalamin. Curves of the subsequent step (formation of cob(II)alamin exhibits more complex curvature and is described by double exponential equation that is typical for two consecutive steps (Fig. 13 b).

The observed rate constants were calculated for the first step ($k_{obs.21}$). Plot of $k_{obs.21}$ versus BSA concentration is linear (Fig. S7) demonstrating the first order of the reaction with respect to BSA concentration. The shape of kinetic curves for the second and third steps does not depend on BSA concentration (Fig. S8). Probably, decomposition of BSA-Cbl(III) complex occurs during these steps, and this does not involve a second protein molecule.

The rate of the first step does not depend on pH in the range between 5 and 6. A slight increase in observed reaction rates was observed upon shift to pH 7, but a further decrease was observed at pH more than 7 (Fig. S9). We were unable to study the kinetics at pH more than 7.5, since, under these conditions, the intensity of spectral changes of thiolato-Cbl(III)-BSA complex formation is very low (Fig. S10), and also, the kinetic curves exhibit a complex shape (Fig. S11) which was difficult to analyze. The increase in reaction rate at pH 6–7 can be explained by deprotonation of thiol groups in BSA (thiolate anion is a stronger nucleophile than thiol; mean pK_a value of thiol groups of different proteins is 6.8 at 25 °C [45]), and further decrease in rate at pH more than 7—by transformation of H_2OCbl to the less reactive hydroxo-form (7.8 at 25 °C [42]).

The rate constant of the second step (k'_{22}) remains unchanged at pH 5–7 and its value is $k'_{22}=(0.086\pm0.010)$ min^{-1} (25 °C). The value of the rate constant of the third step was not determined due to its low reproducibility.

Based on these data, a multi-step mechanism can be suggested for the reaction between H_2OCbl and albumin containing reduced disulfide bonds (Scheme 3). The water moiety on the Co(III) ion is initially substituted by a thiol group of BSA. However, the formed thiolato-complex is unstable and further decomposed. This thiolato-complex is the least stable of all known complexes of Cbl(III) with biological thiols [52] and bulk thiol-containing dendrimers [53], but it is more stable than the complex with hydrogen sulfide [54]. The decomposition of thiolato-Cbl(III)-BSA complex to Cbl(II) includes two steps: the first step likely involves generation of intermediate Cbl(II)-thiyl radical complex, and further the radical leaves coordination sphere of Cbl(II) and dimerizes to disulfide. The possibility of existence of Cbl(II)-thiyl radical complexes has been shown earlier [55]. However, detection of this complex by EPR method is impossible in alkaline and neutral medium [55], which likely explains close similarity between EPR spectra collected during the reaction of H_2OCbl with BSA and that of Cbl(II) (Fig. S5).

Ethoxylation of His residues in BSA does not impair heme or aquacobalamin binding to BSA

The associations of heme, a known ligand of BSA, and aquacobalamin with BSA were investigated in the presence of

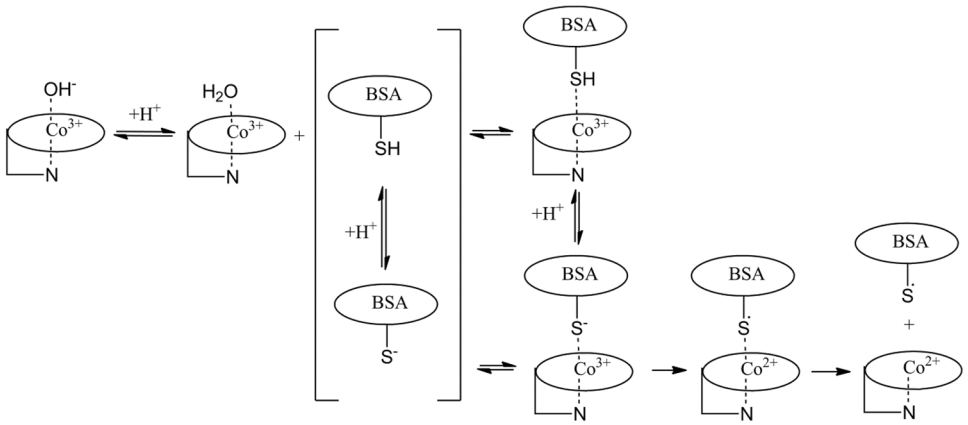

Scheme 3 Mechanism of reaction between H_2OCbl and bovine serum albumin containing reduced disulfide bonds

DEPC, an agent known to block the nitrogen atom of His residues, and to a much lesser extent, to modify Tyr and Lys residues.

Analysis of BSA-heme complex

Formation of BSA-heme was monitored by end-point measurement UV–Vis spectroscopy. First, native BSA or BSA pre-treated with DEPC was incubated with equimolar concentrations of heme. Binding of BSA resulted in a red-shift in the UV–visible spectrum with absorption maxima appearing at 394 and 620 nm, compared to the free tetrapyrrole in buffer that presented absorption maxima at 358, 387 and 614 nm (Fig. S12 A). Interestingly, we found that the spectral properties of BSA-heme complexes formed at 1:1 ratio of protein and ligand are slightly different from the complex formed at higher BSA concentrations, such as for example at 20-fold excess of BSA (Fig. S12 B). Incubation of native or DEPC-treated BSA with hemin in equimolar concentrations generated BSA-heme complexes that are practically identical (Fig. S12 C), suggesting no direct interference of DEPC with heme coordination to BSA. Incubation of native or DEPC-treated BSA with hemin where BSA concentration was higher than that of heme, showed that the presence of excess, unreacted DEPC competed for heme binding to BSA (D), but this effect was eliminated by buffer exchange of the DEPC-treated BSA prior to the addition of heme (E). These results are in line with the reported properties of the human counterpart, HSA-heme complex, whereby blocking of His residues is not expected to have a major impact in heme binding to the protein. While His146 was shown to contribute to heme stabilization in HSA, the crystal structure showed that the tetrapyrrole is tightly held mainly by hydrophobic interactions and by axial coordination with Tyr161 [56]. All these critical amino acid residues are conserved in the bovine albumin utilized in the present study.

Analysis of BSA-H_2OCbl complex and dual tetrapyrrole binding

Binding of BSA to H_2OCbl led to a red-shift in the UV–Visible spectrum (absorption maxima at 358, 506 and 540 nm) compared to free H_2OCbl in buffer (absorption maxima at 351, 499 and 529 nm). Incubation of DEPC-treated BSA with H_2OCbl in equimolar concentrations (Fig. S13 A) as well as at BSA concentration substantially exceeding that of H_2OCbl (20:1 BSA to H_2OCbl, Fig. S13 B), led to modest disruption in BSA-H_2OCbl complex formation, but similarly to the case of heme binding to BSA, this effect was eliminated upon buffer exchange of the BSA-DEPC protein prior to performing binding studies with H_2OCbl (Fig. S13 C).

We next investigated the retention of tetrapyrroles by BSA under native conditions, with subsequent buffer exchange using centrifugal spin-filters with a molecular weight cut-off of 30 kDa (protein complexes are retained, whereas unbound tetrapyrroles are collected in the filtrate). Our data show that H_2OCbl binding to BSA to form a BSA-H_2OCbl complex occurs in the presence of excess BSA. Unlike the case of BSA-heme, incubation of 1:1 BSA-H_2OCbl followed by buffer exchange shows substantial loss of unbound H_2OCbl (Fig. 14a, tube on the left). In contrast, the vast majority of heme was retained by BSA, suggesting distinct stoichiometry of complex formation (Fig. 14a). The BSA-H_2OCbl complex retained by the spin-filter system after 5 cycles of buffer exchange was utilized to test heme binding to pre-formed BSA-H_2OCbl that contains maximal amount of H_2OCbl.

Our data show that presence of maximal amounts of bound H_2OCbl did not preclude subsequent heme binding to BSA (Fig. S14). Under our experimental conditions, H_2OCbl was not displaced from BSA upon heme binding (lack of H_2OCbl displacement was verified by UV–Visible analysis before and after buffer exchange). Subtraction of the initial UV–Vis spectrum of BSA-H_2OCbl from the UV–Vis spectrum of the di-tetrapyrrole complex gave a UV–Vis spectrum

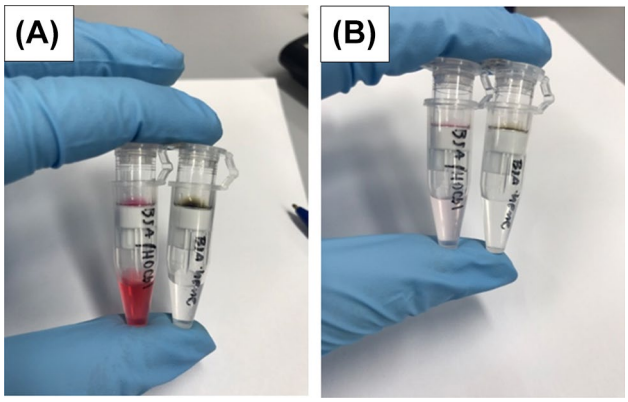

Fig. 14 **a** BSA mixed with equimolar H_2OCbl and flow-through after the first cycle of buffer exchange (filtrate is bright red; left tube). BSA mixed with equimolar heme led to practically complete binding of the tetrapyrrole to BSA, with very little liberation of free heme after the first cycle of buffer exchange (right tube). **b** Shows the BSA-H_2OCbl (left tube) and BSA-heme (right tube) complexes retained by the spin-filter system after 5 cycles of buffer exchange. The experiments were performed in buffer EPPS (40 mM, pH 7.4) supplemented with 150 mM NaCl and 10% glycerol, at room temperature (20 ± 1 °C)

that does not differ markedly from that of authentic BSA-heme complex (Fig. S14 C). This suggests that presence of BSA-bound H_2OCbl does not significantly disturb heme electronics. While binding of heme and cobalamin to BSA was not mutually exclusive under our experimental conditions, the data suggest that BSA interacts with each tetrapyrrole in a distinct manner. Detailed structural characterization and functional implications of this finding await further investigation.

Structural characteristics of the BSA-heme complex and dual binding with H_2OCbl

The crystal structure of the complex between HSA and heme (PDB access codes 1N5U and 1O9X; [56, 57]) showed that the tetrapyrrole is held within its binding pocket mainly via hydrophobic interactions, and H-bonding interactions between the propionate groups of hemin and amino acid residues Arg114, His146 and Lys190 of the protein [56]. In addition, the iron center of the heme moiety is axially coordinated by Tyr161 residue from the protein (Fig. 15) [56]. These amino acid residues are conserved in the structure of BSA, which may enable the same heme binding function by the bovine counterpart, BSA. While heme and cobalamin are structurally and evolutionary related tetrapyrroles [58], vitamin B_{12} has a much larger structure and spatial arrangement compared to heme. Thus, it is possible that heme and cobalamin bind at different sites in BSA. To our knowledge, there are only three reports documenting dual heme and aquacobalamin binding to proteins [59–61]. In these cases, dual binding appears to involve different sites in the respective proteins. Structural elucidation studies are therefore required to unequivocally clarify whether serum albumins possess distinct binding sites for these two tetrapyrroles, or if the well-characterized heme binding pocket of albumin could undergo the required conformational changes to accommodate the bulkier aquacobalamin ligand.

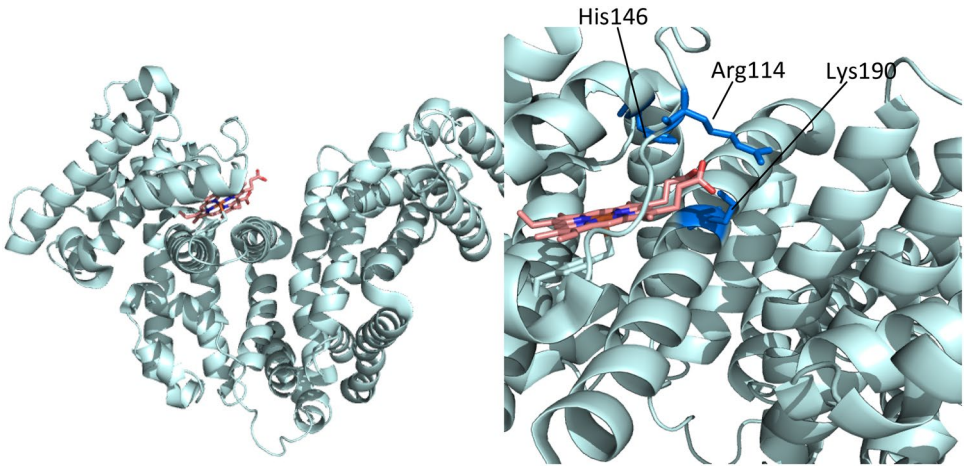

Fig. 15 Structure of human serum albumin (HSA) in complex with heme (PDB 1N5U). Binding of heme by HSA involves axial coordination by Tyr161 and salt-bridge stabilization of the heme propionates by residues Arg114, His146 and Lys190 of the protein [56]. The tetrapyrrole is accommodated in a compact hydrophobic environment. The spatial arrangement seen for the HSA-heme complex would make it unlikely that H_2OCbl could bind to the protein via the same binding site, unless rather substantial conformational changes take place. The images were created with PyMOL(TM) 1.7.6.3—Incentive Product, Copyright (C) Schrodinger, LLC

Conclusions

In this study, we found that aquacobalamin is capable of forming a N-ligated complex (amino) with bovine serum albumin. An additional binding event precedes the coordination of BSA on Co(III) ion. Reduction of disulfide bonds in BSA drastically changes its interaction pathway with H_2OCbl. In this case, coordination of BSA on Co(III) proceeds via thiol group, but the formed thiolate complex is unstable and further decomposes to Cbl(II) and disulfide. Thus, pre-reduced BSA acted as a cobalamin reductase under the experimental conditions of the present study. The binding of H_2OCbl to BSA reduced the yield of CNCbl formation upon reaction with cyanide. While the x-ray structure and biological relevance of the interaction between serum albumin and cobalamin remains to be elucidated, the formation of complexes between cobalamin and non-canonical binders of the micronutrient has been previously documented. For example, under pathological conditions, vitamin B_{12} was found associated to immunoglobulins G and M, and to a lesser extent, presumably to albumin [62]. Our studies showed that binding of cobalamin to BSA modified the reactivity of the micronutrient. This could be a mechanism to limit unwanted side reactions of the redox active cobalamin when the binding capacity of its cognate transport proteins in plasma, namely, transcobalamin and haptocorrin, has been exceeded. Results from this study showed that binding of heme and cobalamin to BSA are not mutually exclusive under our experimental conditions. This expands the repertoire of ligands that albumin can accommodate in concert.

Acknowledgements This work was supported by the Russian Foundation for Basic Research (Project No. 16-33-00025) to IAD and by the Russian Science Foundation (Agreement No. 14-23-00204) to OIK.

References

1. Dereven'kov IA, Salnikov DS, Silaghi-Dumitrescu R, Makarov SV, Koifman OI (2016) Coord Chem Rev 309:68–83
2. Knapton L, Marques HM (2005) Dalton Trans 889–895
3. Chemaly SM, Brown KL, Fernandes MA, Munro OQ, Grimmer C, Marques HM (2011) Inorg Chem 50:8700–8718
4. Borron SW, Baud FJ, Barriot P, Imbert M, Bismuth C (2007) Ann Emerg Med 49:794–801
5. Sauer SW, Keim ME (2001) Ann Emerg Med 37:635–641
6. Gherasim C, Lofgren M, Banerjee R (2013) J Biol Chem 288:13186–13193
7. Nielsen MJ, Rasmussen MR, Andersen CBF, Nexø E, Moestrup SK (2012) Nat Rev Gastroenterol Hepatol 9:345–354
8. Banerjee R, Ragsdale SW (2003) Annu Rev Biochem 72:209–247
9. Fedosov SN, Berglund L, Fedosova NU, Nexø E, Petersen TE (2002) J Biol Chem 277:9989–9996
10. Seetharam B, Yammani RR (2003) Expert Rev Mol Med 5:1–18
11. Wuerges J, Garau G, Geremia S, Fedosov SN, Petersen TE, Randaccio L (2006) Proc Natl Acad Sci USA 103:4386–4391
12. Banerjee R (2006) ACS Chem Biol 1:149–159
13. Kim J, Gherasim C, Banerjee R (2008) Proc Natl Acad Sci USA 105:14551–14554
14. Hannibal L, Kim J, Brasch NE, Wang S, Rosenblatt DS, Banerjee R, Jacobsen DW (2009) Mol Genet Metab 97:260–266
15. Kim J, Hannibal L, Gherasim C, Jacobsen DW, Banerjee R (2009) J Biol Chem 284:33418–33424
16. Peters JT, Stewart AJ (2013) Biochim Biophys Acta 1830:5351–5353
17. Turell L, Radi R, Alvarez B (2013) Free Radic Biol Med 65:244–253
18. Petitpas I, Grüne T, Bhattacharya AA, Curry S (2001) J Mol Biol 314:955–960
19. Pavićević ID, Jovanović VB, Takić MM, Penezić AZ, Aćimović JM, Mandić LM (2014) Chem Biol Interact 224:42–50
20. Novotná P, Urbanová M (2015) Biochim Biophys Acta 1848:1331–1340
21. Goncharova I, Orlov S, Urbanová M (2013) Chirality 25:257–263
22. Lebedeva NSh, Gubarev YA, Lyubimtsev AV, Yurina ES, Koifman OI (2017) Macroheterocycles 10:37–42
23. Zhang W, Zhang L, Ping G, Zhang Y, Kettrup A (2002) J Chromatogr B 768:211–214
24. Zhao P, Huang J-W, Ji L-N (2012) Spectrochim Acta Mol Biomol Spectrosc 88:130–136
25. Watanabe S, Sato T (1996) Biochim Biophys Acta 1289:385–396
26. Baker ME (2002) J Endocrinol 175:121–127
27. Yamasaki K, Chuang VTG, Maruyama T, Otagiri M (2013) Biochim Biophys Acta 1830:5435–5443
28. Yang F, Zhang Y, Liang H (2014) Int J Mol Sci 15:3580–3595
29. Bujacz A (2012) Acta Cryst D68:1278–1289
30. Hou H-N, Qi Z-D (2008) Yang Y-WO, Liao F-L, Zhang Y, Liu Y. J Pharm Biomed Anal 47:134–139
31. Li D, Zhang T, Xu C, Ji B (2011) Spectrochim Acta Mol Biomol Spectrosc 83:598–608
32. Makarska-Bialokoz M (2017) Acta Mol Biomol Spectrosc 184:262–269
33. Obeid R, Fedosov SN, Nexo E (2015) Mol Nutr Food Res 59:1364–1372
34. Taylor RT, Hanna M (1970) Arch Biochem Biophys 141:247–257
35. Lien EL, Wood JM (1972) Biochim Biophys Acta 264:530–537
36. Satterlee JD (1980) Inorg Chim Acta 46:157–166
37. Barker HA, Smyth RD, Weissbach H, Munch-Petersen A, Toohey JI, Ladd JN, Volcani BE, Wilson RM (1960) J Biol Chem 235:181–190
38. Ellman GL (1959) Arch Biochem Biophys 82:70–77
39. Hannibal L, Collins D, Brassard J, Chakravarti R, Vempati R, Dorlet P, Santolini J, Dawson JH, Stuehr DJ (2012) Biochemistry 51:8514–8529
40. Jarolim P, Lahav M, Liu SC, Palek J (1990) Blood 76:2125–2131
41. Mendoza VL, Vachet RW (2009) Mass Spectrom Rev 28:785–815
42. Xia L, Cregan AG, Berben LA, Brasch NE (2004) Inorg Chem 43:6848–6857
43. Bui TTT, Salnikov DS (2017) Dereven'kov IA, Makarov SV. Russ J Phys Chem A 91:658–661
44. Hannibal L, Lysne V, Bjorke-Monsen AL, Behringer S, Grunert SC, Spiekerkoetter U, Jacobsen DW, Blom HJ (2016) Front Mol Biosci. https://doi.org/10.3389/fmolb.2016.00027
45. Grimsley GR, Scholtz JM, Pace CN (2009) Protein Sci 18:247–251
46. Tanford C (1952) J Am Chem Soc 74:211–215
47. Hayward GC, Hill HAO, Pratt JM, Vanston NJ, Williams RJO (1965) J Chem Soc 6485–6493

48. Dereven'kov IA, Salnikov DS, Makarov SV, Surducan M, Silaghi-Dumitrescu R, Boss GR (2013) J Inorg Biochem 125:32–39
49. Lakowicz JR, Weber G (1973) Biochemistry 12:4161–4170
50. Ware WR (1962) J Phys Chem 66:445–448
51. Rombouts I, Lagrain B, Scherf KA, Koehler P, Delcour JA (2015) Sci Rep. https://doi.org/10.1038/srep12210
52. Suto RK, Brasch NE, Anderson OP, Finke RG (2001) Inorg Chem 40:2686–2692
53. Sommer P, Uhlich NA, Reymond J-L, Darbre T (2008) ChemBioChem 9:689–693
54. Salnikov DS, Kucherenko PN (2014) Dereven'kov IA, Makarov SV, van Eldik R. Eur J Inorg Chem 2014:852–862
55. Ramasamy S, Kundu TK, Antholine W, Manoharan PT, Rifkind JM (2012) J Porphyr Phthalocyanines 16:25–38
56. Wardell M, Wang Z, Ho JX, Robert J, Ruker F, Ruble J, Carter DC (2002) Biochem Biophys Res Commun 291:813–819
57. Zunszain PA, Ghuman J, Komatsu T, Tsuchida E, Curry S (2003) BMC Struct Biol. https://doi.org/10.1186/1472-6807-3-6
58. Yin L, Bauer CE (2013) Phil Trans R Soc B. https://doi.org/10.1098/rstb.2012.0262
59. Eakanunkul S, Lukat-Rodgers GS, Sumithran S, Ghosh A, Rodgers KR, Dawson JH, Wilks A (2005) Biochemistry 44:13179–13191
60. de Orué Lucana DO, Fedosov SN, Wedderhoff I, Che EN, Torda AE (2014) J Biol Chem 289:34214–34228
61. Vermeulen AJ, Bauer CE (2015) J Bacteriol 197:2694–2703
62. Bowen RAR, Drake SK, Vanjani R, Huey ED, Grafman J, Horne MK (2006) Clin Chem 52:2107–2114